D13

N79-27083

EXPERIMENTAL STUDY OF THE FLIGHT ENVELOPE AND RESEARCH OF SAFETY REQUIREMENTS FOR HANG-GLIDERS

by Claudius LA BURTHE

Head of Aircraft Section
Aerospace Mechanics Division
Systems Department

Office National d'Etudes et de Recherches Aérospatiales (ONERA)
92320 Châtillon (France)

◆

ABSTRACT

Hang gliding was born as a popular sport in France in the 70's. After a period of observation, French Officials decided that hang gliders were no longer to be considered as toys, but as a new kind of aircraft. Then, French Government funded a two years' research contract at ONERA on the safety of hang-gliders, in an attempt to set up the most adequate acceptance rules.

S1, 8 x 16 meters wind-tunnel of Chalais-Meudon near Paris, was used for two series of full scale tests, with 15 different gliders, including two-seaters, and most of them with a dummy pilot. A six component instrumentation provided lots of aerodynamic data. Flow visualization was used and showed quite unexpected air flows.

The calculated basic performances were checked in real flight by the author, with some of the same gliders as used in the tunnel.

The flight mechanics computations were then completed, providing both the flight envelopes wit all sorts of limits and a fairly precise idea of the influence of several parameters, such as pilot's weight, wing settings, aeroelasticity, etc... The particular problem of luffing dives was thoroughly analysed, and two kinds of causes were exhibited in both the rules of luffing and aeroelastic effects. The general analysis of longitudinal stability showed a strong link with fabric tension, as expected through Nielsen's and Thwaites' theory. Fabric tension strongly depending upon aeroelasticity, that parameter was found to be the most effective design one for positive stability.

Lateral stability was found to be very similar in all gliders except perhaps the cylindro-conical. The loss of stability happens in roll at low angle of attack, whereas it happens in yaw at high angle. Turning performance was a bit surprising, with a common maximum value of approximately 55° of bank angle for a steady turn.

Structure calculations began on the basis of an isostatic technique which did not succeed because the leading-edges, keel, and cross-spar were separated. Then, a linear finite elements technique was used and gave very adequate results for normal loadings, since the comparison with both flight and ground tests was very satisfactory. The prediction of ultimate loadings and breaking of the structure is less precise, and would possibly require a non-linear computation because of the bendings.

During the research, all reports about significant casualties happening in France were analysed at ONERA and were of great help in the direction of the study.

The conclusions of the research are, first that none of the normal aeronautical requirements would apply to the case of hang-gliders. One good example would be the stall, which is the base of a good half of a normal aircraft certification. A hang glider would possibly require the half of the certificator's attention on its maximum diving speed. As

far as certification means are concerned, it is intended to make an aerodynamic-test-vehicle which would be devoted only to development and stability checks. A structural acceptance could be delivered on the basis of a calculation, plus ground-testing, using the ONERA method.

But probably the most important impact of the research in terms of hang-gliders flight safety was the dissemination of this information to French instructors and pilots.

SYMBOLS

AOA angle of attack
C_D drag coefficient
C_{D0} drag coefficient at $\alpha = 0$ (linearized)
C_L lift coefficient
$C_{L\alpha}$ derivative : $dC_L/d\alpha$ (linearized), lift gradient
$C_{\ell,\beta}$ rolling moment due to sideslip-coefficient
C_M pitching moment coefficient
C_{M0} pitching moment coefficient at $\alpha = 0$ (linearized)
$C_{M\alpha}$ derivative $dC_M/d\alpha$ (linearized)
$C_{M\beta}$ pitching moment due to sideslip-coefficient
$C_{N\beta}$ yawing moment due to sideslip-coefficient
F force exerted by the pilot on the control bar ($F > 0$ corresponds to a nose-up action)
G center of gravity of the vehicle
ℓ aerodynamic chord (length of the keel)
L/D fineness ratio
O center of the glider (at the crossing of keel and cross-par)
O,X,Y,Z wing axes
$\vec{R}$ resulting aerodynamic force on the glider
V relative air velocity
V_{stall} stalling speed
Z_G height of center of gravity, wing axis (see fig.)
α angle of attack (in degree)
α_β corresponding to maximum L/D
α_K corresponding to the kink point on $C_M(\alpha)$ curve
α_{Luff} corresponding to onset of luffing if α decreases
$\alpha_{min\ sink}$ corresponding to minimum sink speed
α_{V-} corresponding to maximum of $\sqrt{C_L^2 + C_D^2}$ (minimum flying speed)
β sideslip
$\Delta_E\alpha = \alpha_{V-} - \alpha_{Luff}$
$\Delta_S\alpha = \alpha_{V-} - \alpha_K$
δ angle between wing-axis OZ and pilot strap (see fig.) ($\delta > 0$ corresponds to a nose-up action)
λ aspect ratio

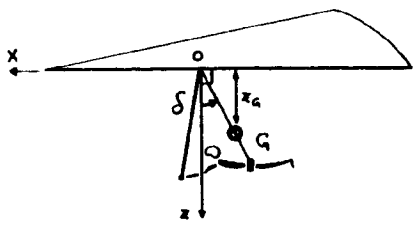

Δ aircraft in trim with control bar free ($F = 0$)
P luffing limit
maneuvering limit (max length of the pilot's arms)
force limit (25% of pilot's weight)
loss of roll control
loss of yaw control

INTRODUCTION

In France, hang gliding started to be a popular sport in 1973, when a national association (FFVL) was born. There were some hundreds of people flying, almost all claiming to be instructors! As usual, some dramatic accidents focused everyones attention on hang gliding, and fairly soon, many flying places became very crowded. Some of them were closed because of the problems created by the people watching and their motor-cars. But the aeronautical authorities were reluctant to consider them as real aircraft, and preferred initially to classify them as beach games, in order not to have to certify them.

After two years, it was clear that a new kind of aircraft was flying French skies, and something had to be done about its flying safety. The DGAC (equiv. to F.A.A.) funded a two years' research at ONERA about the flying envelope of ultralight hang-gliders, and requested advice for future specifications.

In order to avoid difficult similarity problems due to the slackness of fabric, it was decided to go through scale 1 tests in S1 Meudon wind-tunnel. The gliders used covered different shapes from the standard Rogallo to the Fledgling 1.

Somewhat unexpected results were obtained, and it was decided to check the main performances in flight, which was done successfully.

Then, the flight mechanics computations were completed, and highlighted some very interesting and specific features of these vehicles.

At the same time structural calculations were undertaken, and constantly cross-checked with in-flight and ground-test measurements.

But the determination of handling, performance and structure specifications remains difficult because of the numerous non-linearities encountered in the problem, and the difficulty of defining adequate demonstrations for the manufacturers.

AERODYNAMICS

Wind-tunnel testing of a sail-wing mock-up raises difficult scale effect questions. Therefore ONERA decided to use S1 Meudon, which allows scale 1 tests of hang-gliders, thanks to its 16 x 8 m elliptic facility. Nevertheless, the study is not necessarily free of Reynolds problems, as the paragliders' flying speeds places their Reynolds number in the range of 1 to 8 million. This could explain a good part of the scattering found in the tunnel results.

Two series of one month tests were performed with 15 different gliders covering the shapes shown on figure 1.

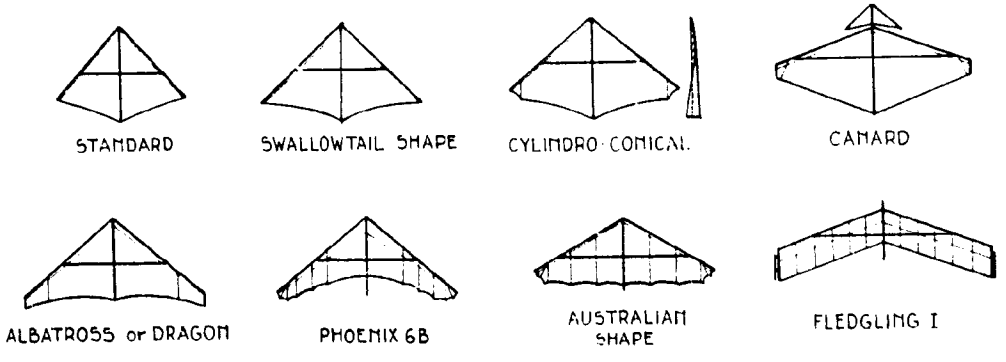

Fig. 1 – Survey of the shapes of gliders used.

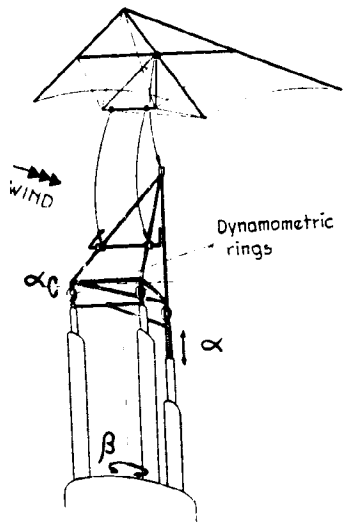

Fig. 2 – Wind tunnel arrangement.

The mounting is basically made of a tetrahedral tubing (fig. 2), fixed on three vertical masts, through three dynamometric rings. The glider is fixed by means of clutches :

a) at its "center", on the top of the tetrahedron,

b) at the control bar on both front struts.

The rear mast ends with a screw-jack which provides adjustment of the angle-of-attack. The whole of the mounting can rotate about a vertical axis for sideslip setting.

All tests were made under static conditions, and all measurements had to be strongly filtered because of the effects of wire and fabric vibrations.

Flow visualization revealed quite unexpected air flows, in that :

– no wing-tip vortex was found around cruise A.O.A. ($\sim 20°$),

– a fairly high vorticing activity was found in the center-part of the wing, in spite of sweep angles ($< 45°$) well below the admittec minimum value of $\sim 52°$ for a vortex flow to be organised over the wing. This is almost certainly due to wing twist, which is surprisingly always near to $20°$, thus preventing early separation.

Fig. 3 a) and b) show the results of visualizations respectively made with tufts and smoke, in the tunnel and in flight at all AOAs. Fig. 4 indicates the general flow around the wing at cruise angle of attack.

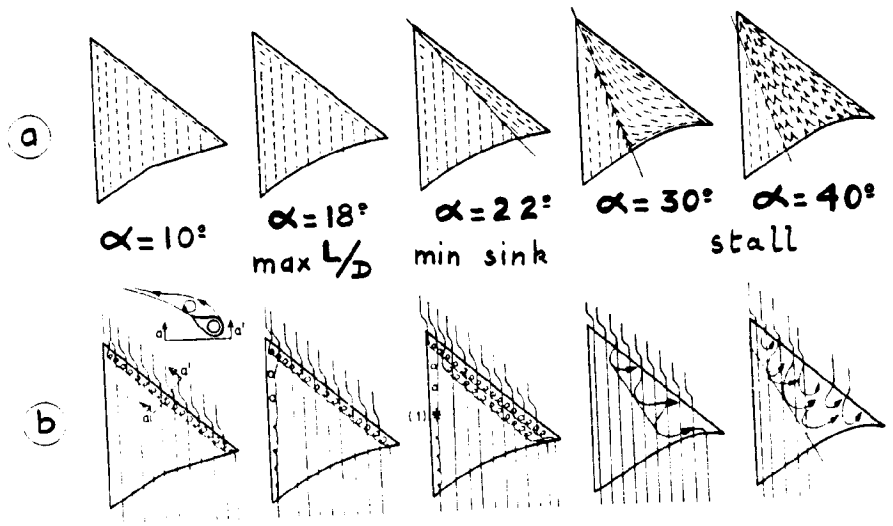

Fig. 3 – Flow visualization with tufts (a) and smoke (b).

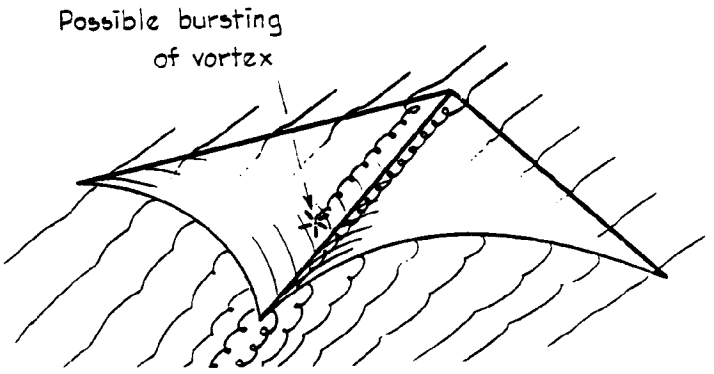

Fig. 4 – Flow visualization, cruise A.O.A.

Two important consequences have to be mentioned. The aerodynamic loading vs. wing-span is less severe than expected through a two-dimensional theory. The flow above described remains as long as the shape of the fabric is self-adapting to the angle of attack, i.e. between luffing angle and approximately 25°. The latter characteristic provides unique capabilities to Rogallo wings in that their flying envelope is significantly increased (by an angle of 10° or more) with regard to a normal "rigid" aircraft. Fig. 5 shows the flying envelopes infered from the following definition : the usable angles-of-attack $\Delta_{E\alpha}$ are limited by luffing: α_{luff} and stall: $\alpha_{\sqrt{max}}$.

	α°_{luff}	$\alpha^\circ_{L/D\ max}$	L/D max	α° min sink	α°_K	$\Delta_S\alpha^\circ$ $(\alpha_{\sqrt{}} - \alpha_K)$	$\alpha^\circ_{\sqrt{}}$	$\Delta_{E\alpha}{}^\circ$ $(\alpha_{\sqrt{}} - \alpha_{luff})$
Standard	7	20	4.3	23	30	9	39	32
Swallowtail	9	23	5.5	24	30	6	36	27
Cylindro con.	9	18	4.9	24	31	–1	30	24
Canard	12	24	4.1	32	–	–	36	24
Albatross	1	16	5.5	19.5	27	0	27	26
Phoenix 6B	<6	18	5.9	21	29	3	32	>26
Australian	8	24	5.0	27	31	1	32	24
Fledgling	–5	12.5	7.6	14	–	–	20	25

Fig. 5 – Key A.O.As used in defining the flight envelopes.

Under these conditions, one could expect to find numerous non-linearities in the aerodynamic data. In fact, there are many, but curiously, the lift coefficient remains pretty linear against α (Fig. 6) as long as the fabric is free of luffing and far from stall conditions, which means able to adapt its own shape to the proposed angle of attack. The local linearity allows drawing a graph of $C_{L\alpha}$ against aspect ratio λ for all the gliders in the study (Fig. 7). Then it is possible to compare data of different origins : Fig. 8 and refs. [2, 3, 4, 5, 6].

But C_L is the only coefficient to behave so, and unfortunately the non linearities of the pitching moment C_M are very strong. Fig. 6 shows typical results obtained at constant wind speed in the tunnel. But these do not represent the actual conditions of flying, because the variations of speed induce variable loads on the aluminium structure, which is very flexible . Consequently, the shapes of the wings, mainly the billow, are modified, up to the point where it was found essential to make tunnel tests at different speeds (precisely 3 speeds in the range of 8 to 20 m/s or 18 to 45 m.p.h.). Fig. 6 shows one example of the necessary interpolation. The impact will be analysed in the discussion of longitudinal stability.

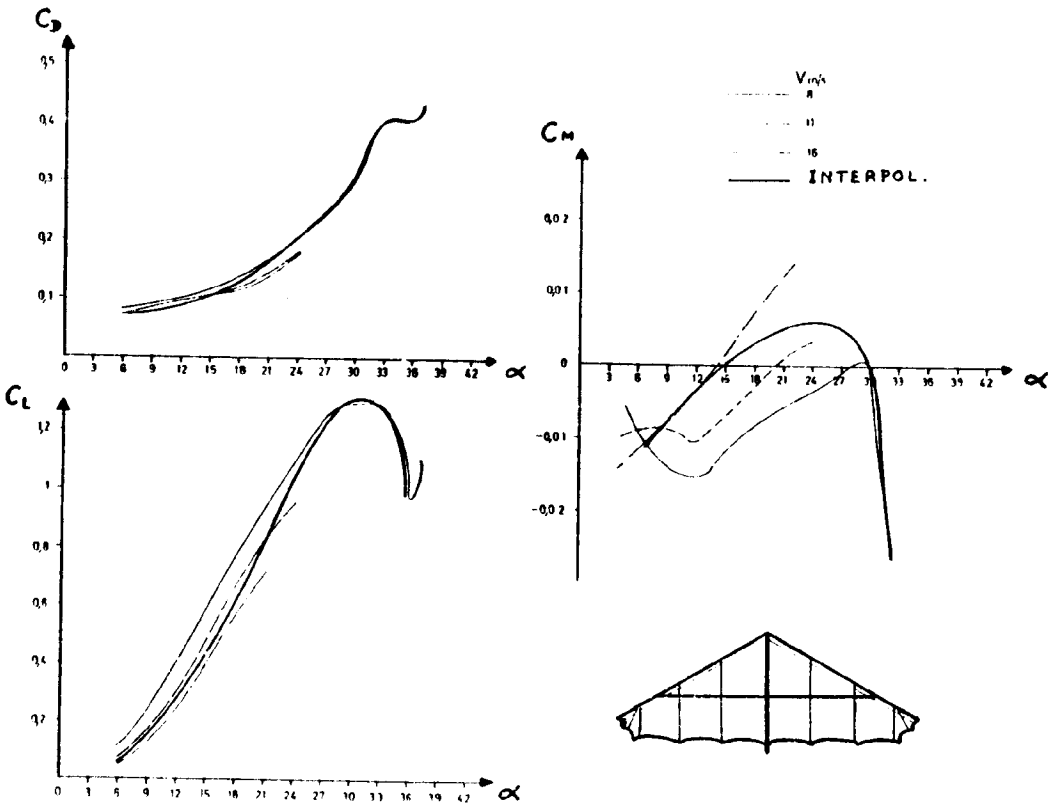

Fig. 6 – Typical tunnel results.

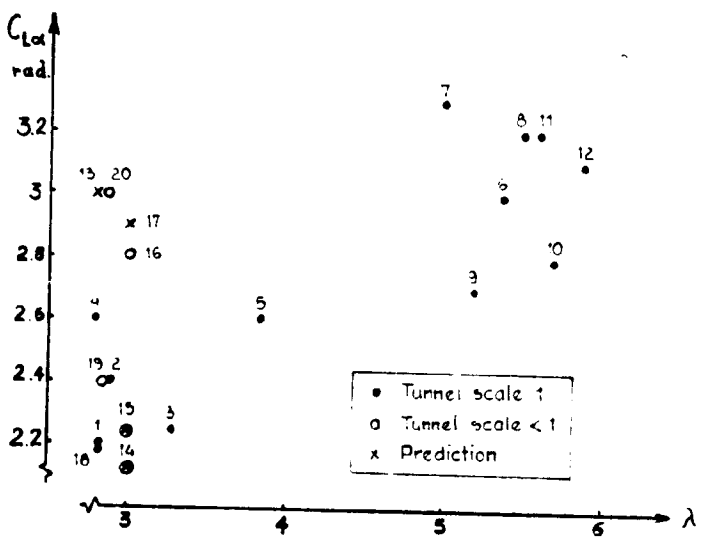

Fig. 7 – Lift gradient vs. aspect ratio.

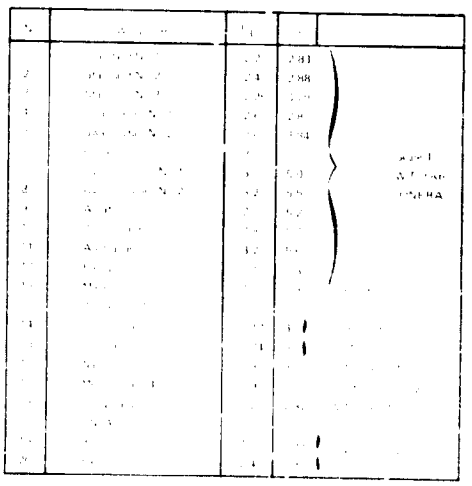

Fig. 8 – Origins of lift gradients used in fig. 7.

The angles-of-attack limiting the flying envelope, as mentioned above, have to be discussed. The correlated analysis of the wing shape and pitching moment at low angle provides a clear explanation of the so-called luffing-dives. Fig. 9 shows how quickly and how far the center of pressure moves back when α decreases, in conjunction with a partition of the sail into two parts :

a) one immediately downstream of the leading edges which flutters and does not provide any lift,

b) the central part, which is inflated, and probably lifted up by the nose vortices, and which gives a local lift, applied in the rear part of the wing.

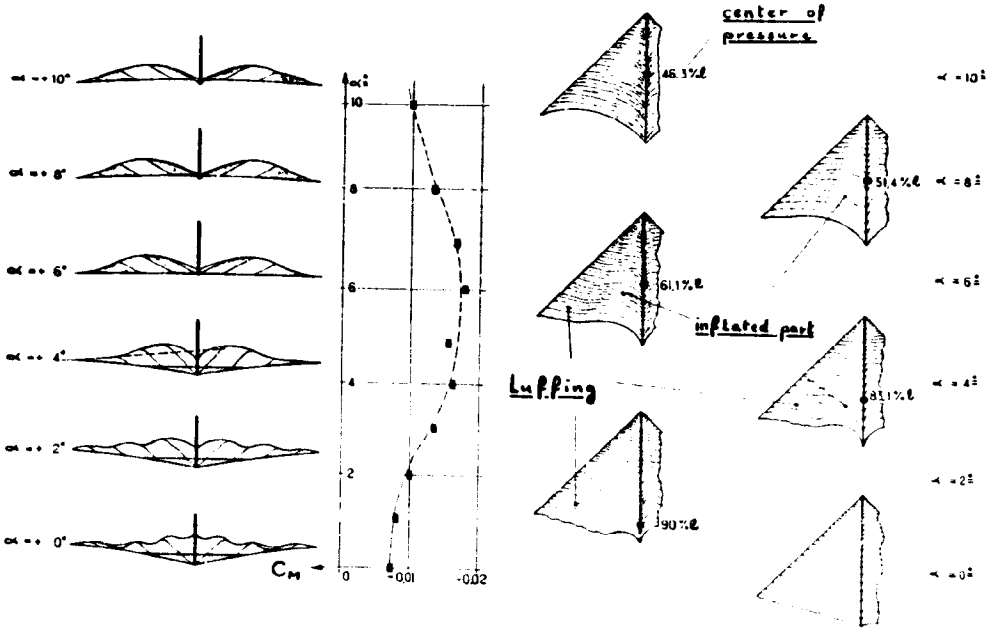

Fig. 9 – Mechanism of "aerodynamic luffing"

This phenomenon is typical of conical wings, obviously very dangerous, and of increased severity with increased length of the keel. It could explain many accidents, and will be called "aerodynamic luffing" in this paper. One must keep in mind that it happens at positive, but admittedly small, AOA, precisely when the billows are not fully inflated. It should not be confused with the cause of tumbling which is discussed below.

At negative AOA, the sails tend to invert, but are partly restrained by the cross-spar (if there is one). In that case, the shape indicated on Fig. 10 provides a very violent nose-down pitching moment which is able to launch the wing in a permanent motion, called **tumbling** [7].

On the other end, the stall can't be defined as precisely as on a normal aircraft, because of the very important wing twist. This will necessarily prevent abrupt flow-separation, and systematically provide a nose-down reaction of the glider. Thus a Rogallo glider may be fundamentally safe at stall. The stall conditions may be difficult to define up to the point that a reference to V_{stall} may no longer be possible. Actually, two events go along with stall. In an increase of α , one first meets a marked kink in the $C_M = f(\alpha)$ curve at α_k (discontinuity on $d C_M / d\alpha$). But lift continues to increase up to its maximum obtained at $\alpha_{V^{max}}$. Fig. 5 shows the values of $\Delta_S\alpha = \alpha_{V^{max}} - \alpha_k$ which are of interest in forecasting the behaviour of the glider at stall. Thus a good correlation was obtained between forecast and flight on the stalls obtained after quasi-static slow-downs, the severity of the stall being less with increased gap between both events (increased $\Delta_S\alpha$). But this does not apply to most of the stalls actually occuring in flight, which are more or less dynamic ones, and often more severe than expected. A good study remains to be done on the

influence of the local magnitude of $C_{L\alpha}$ on the severity of the stall at a given $\Delta_s\alpha$.

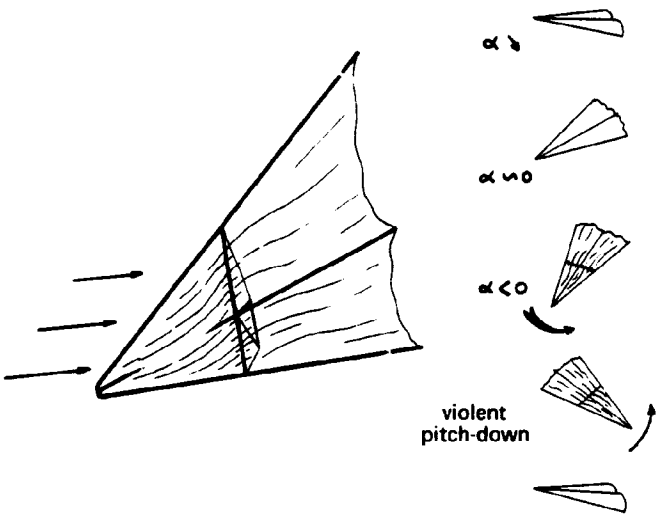

Fig. 10 – Tumbling.

FLIGHT MECHANICS

The first polar curves obtained in the tunnel provided surprisingly high minimum flying speeds, as well as scattered typical performance speeds (minimum sink and maximum L/D, as presented in fig. 5). The minimas were approximately but successfully checked in flight, using a simple but effective instrumentation, which provided through telemetry : air-speed, A.O.A., 3-axis-accelerometers, and two structural stresses (Fig. 11 and 12 give the calibrations). As an indirect consequence of that verification, we had to consider that a hang-glider is often flying in unsteady conditions, for example at take-off, landing, initiation of a turn, stall. This is due to the effects of the accelerated air-mass around the glider, which probably can't be neglected, and puts a severe limitation on the validity of quasi-static models.

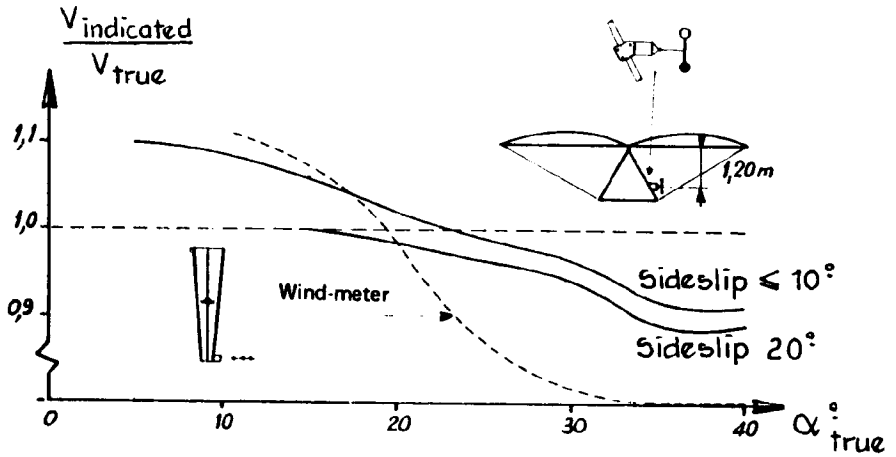

Fig. 11 – Calibration of spoon anemometer.

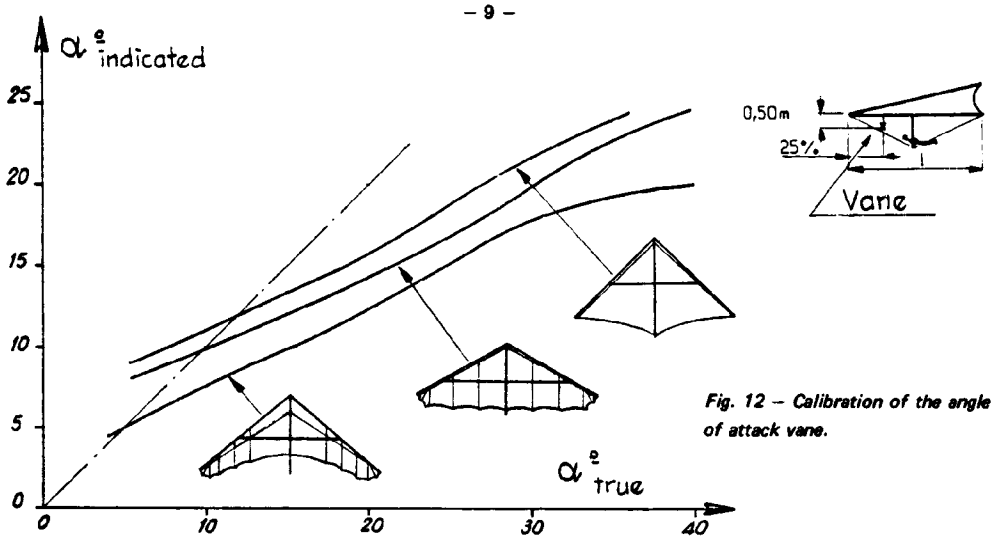

Fig. 12 – Calibration of the angle of attack vane.

The overall verification of the calculated performance allowed the estimation of the origins of drag. Fig. 13 shows the little contribution of pilot's body, but the high level of friction drag.

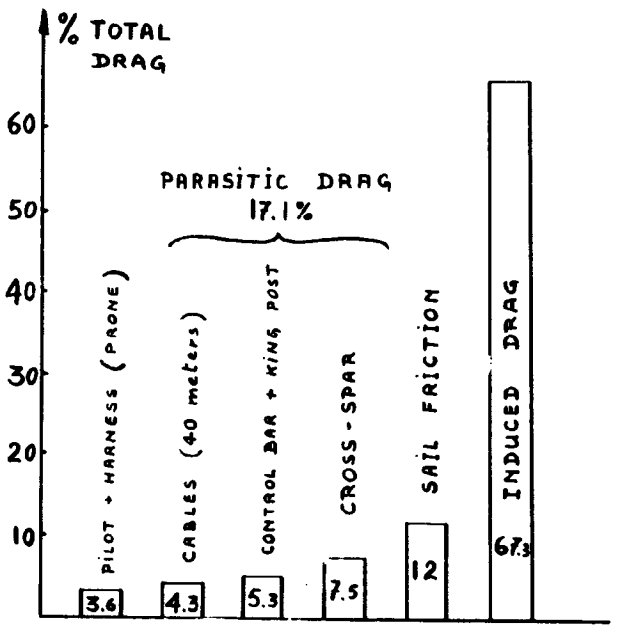

Fig. 13 – Contribution to total drag (typical wing, $C_{Do} = 0.06$, $L/D = 5$, $V = 10$ m/s).

There is no doubt that the most critical problem of hang-gliders is longitudinal stability. It was explained above that non-linearities are present everywhere in the aerodynamic data, especially if aeroelastic effects are taken into account. One consequence is that it is not possible to define an aerodynamic center, which would require constant values of $C_{L\alpha}$ and $C_{M\alpha}$. Another particular feature of hang-gliders is the lowered center of gravity, which introduces an effect of drag on longitudinal stability. Remembering the rule of positive stability which applies to a normal flying wing : $CM_o < 0$, it might be generalized to a hang-glider, whose aerodynamics would be linear, if

$$C_{Mo} < -\frac{z_4}{l} C_{Do}$$

assuming z_4 constant (the calculation has to be made in body-axis, using Lilienthal polar curve).

In order to clarify the problem, fig. 14 shows how the actual resulting aerodynamic force $\vec{R}$ varies in body axis. The necessity of equilibrium fixes the center of gravity of the vehicle at a given location for a given α.

If the aerodynamic data C_D C_L C_M were linear, or at least conventional, the intersection G of $\vec{R}$ and a circle centered in O would vary regularly. As it is not the case, the displacement of point G moves in an odd manner against α .

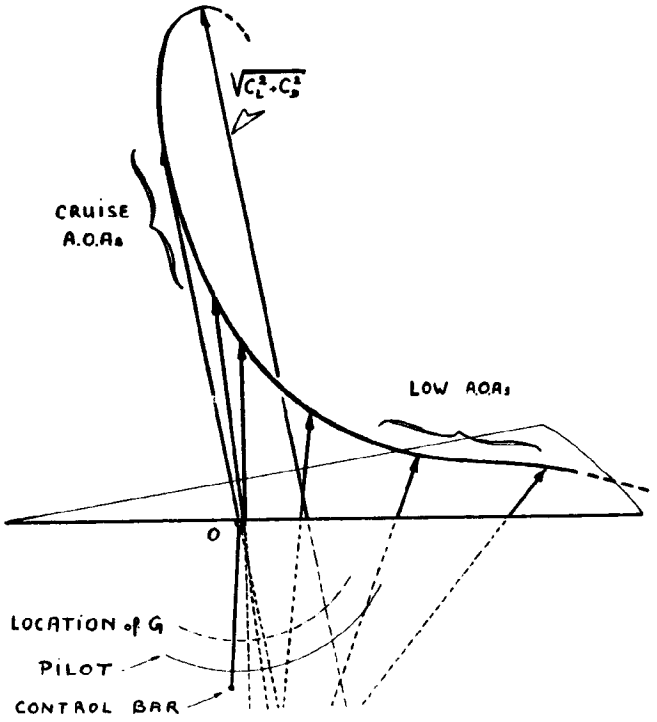

Fig. 14 – Location of resulting aerodynamic force in body axis (unstable wing).

The problem of longitudinal stability having no analytical solution, a numerical computation was performed, giving both pilot's forces F and displacements δ in body-axis against α . Analysing the significance of these curves shows that :

a) "effort"– or "control bar free" stability $F(\alpha)$ is typical of stability about O, pilot's weight being a pure pitching moment generator, as seen on figure 15,

b) "displacement"– or "control bar fixed" stability $\delta(\alpha)$ is typical of stability about G, as seen on figure 16.

The latter being necessarily smaller, "control bar free" stability is to be prefered as a safety criterion, which would write $dF/d\alpha$.

Computations were so organized that $F(\alpha)$ was the final result to be obtained. As it is rather easy to measure pilot forces against speeds F(V) in flight, this was used as means of checking the whole of the calculations. Comparisons are shown on figure 17.

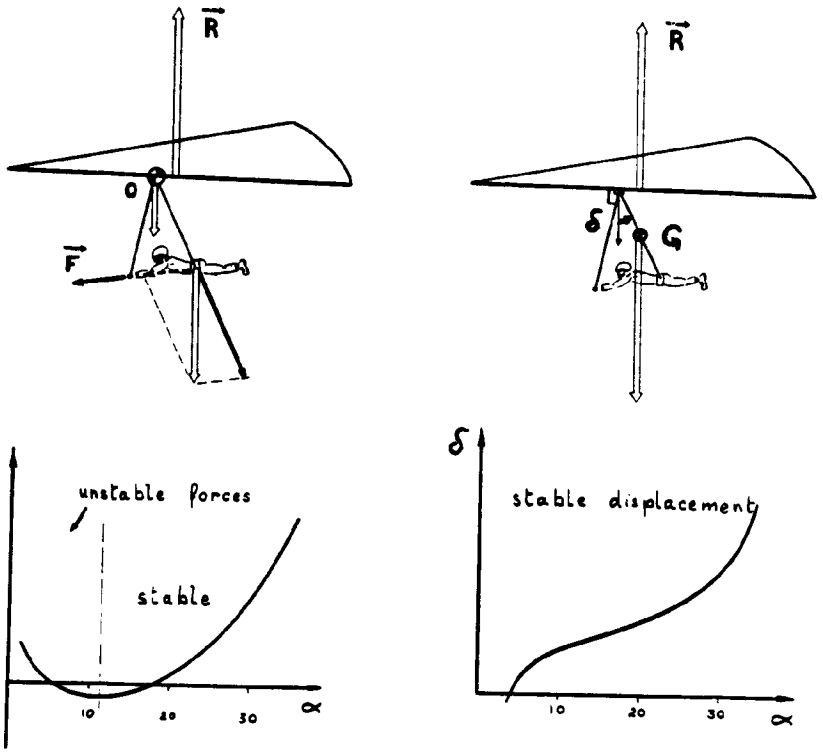

Fig. 15 – "Control bar free" stability.

Fig. 16 – "Control bar fixed" stability.

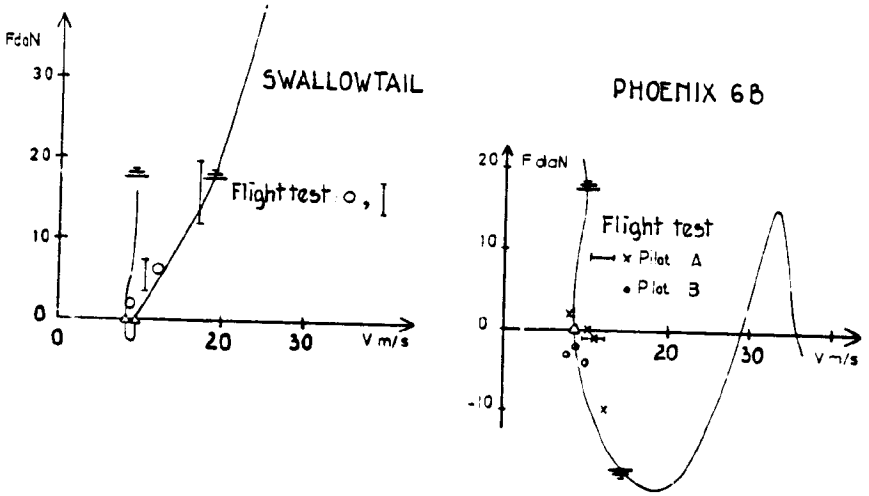

Fig. 17 – Comparison of flight test results vs. computations.

But many of the gliders in the study still presented significant instabilities at low A.O.A. in spite of having rather short keels. Looking at pitching moment curves obtained at different tunnel speeds proved that aeroelastic effects often have a negative influence on longitudinal stability at low A.O.A. Figure 18 shows this and gives a physical explanation, which was found to be applicable to a wide majority of gliders. The inwards displacement of the front part of the leading-edges loosens the fabric around the nose (fig. 19), and local lift drops dramatically, according to Thwaites' and Nielsen's theory on the behaviour of sail wings [8, 9]. This is a second explanation of the well known divergent luffing drives, and will be called **"aeroelastic luffing"** as opposed to the "aerodynamic luffing" described previously. Fortunately, this dangerous effect can be easily suppressed by anchoring one end of the deflectors in the middle of the bending part of the leading edges, as shown on figure 18. But, aeroelastic effects on longitudinal stability will certainly remain important, and thus become a very effective design parameter for the manufacturer.

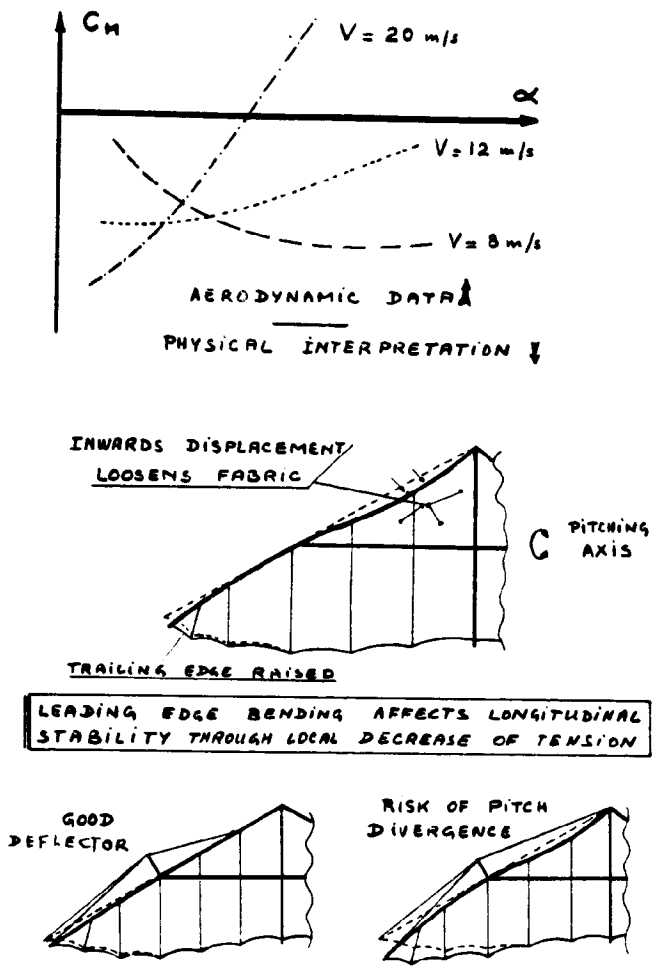

Fig. 18 – "Aeroelastic luffing".

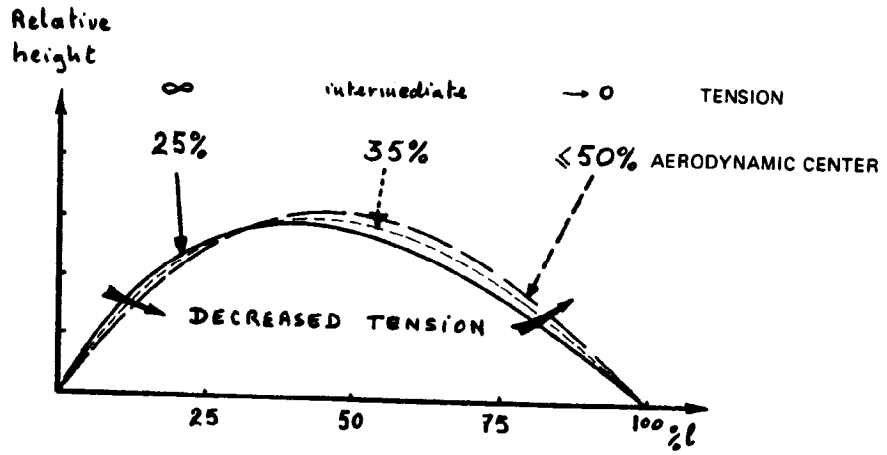

Fig. 19 – Two-dimensional theory of fabric airfoils (Thwaites & Nielsen).

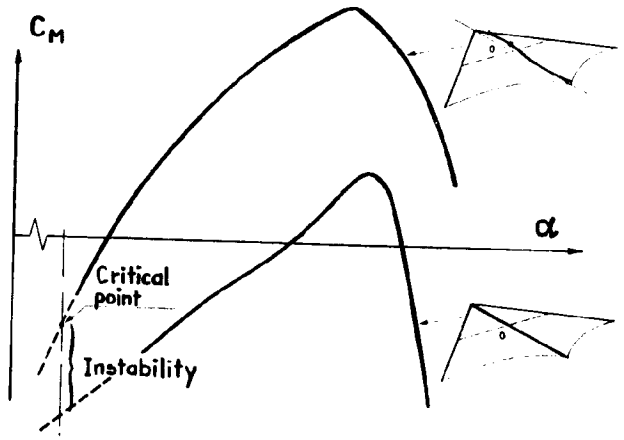

Fig. 20 – Typical effect of keel camber.

A more generalized use of Nielsen's and Thwaites' theory shows that there is a strong relationship between longitudinal stability and flying speed. Speed creates tension, and tension governs shape of the profile, as shown on figure 19. Consequently a variation of speed can result in a significant displacement of the center of pressure in the wrong direction.

Another feature is favourable to a positive longitudinal stability : the keel camber, as shown on figure 20.

Lateral stability and handling was found curiously more or less similar with all gliders in the study. It was first determined in flight that normal flying allows normal increments of 10° of sideslip, whereas ultimate manoeuvers can result in $\beta = 30°$.

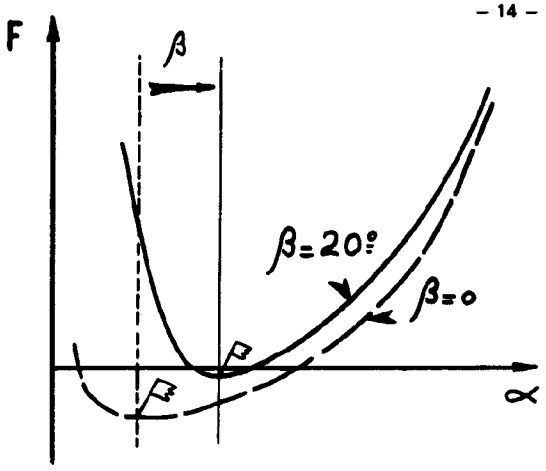

Fig. 21 – Effect of sideslip β on onset of longitudinal instability.

Laterally, the most important result is the general magnitude of $C_{M\beta}$, which corresponds to a marked pitch-down moment. Common sideslip effect is to raise the beginning of longitudinal instability by several degrees (fig. 21). This results in a modification in the shape of the forward wing due to sideslip : the fabric tends to flatten itself downstream of the leading-edge, and the application of lift moves back. The effect on the shape of the other wing is negligible in terms of camber. This results in a high risk of "tucking into a turn" when it is initiated at very low speed, and could explain several accidents.

Lateral stability itself was analysed by means of an old fashioned criterion which looks like the **"spiral stability"** one.

Its use demonstrated that all gliders in the study would become laterally unstable at both ends of A.O.A. envelope because of loss of yawing stability ($C_{N\beta}$) at high A.O.A., and because of loss of rolling stability ($C_{\mathcal{L}\beta}$) at low A.O.A. It was surprising to find such a result, which can't be generalized without care.

Turning performance was also surprising. The turning equations normally used for aircraft capable of making horizontal turns are not adequate for the case of a glider with poor L/D, which is only capable of a helicoidal motion. An adequate set of equations was used and resulted in the performances given in figure 22. Again, they are rather similar with all gliders because of the little scattering in maximum L/D. The most important ones are:

a) it is not possible to make a steady turn if bank angle is bigger than ~ 60° ;

b) at a given lower bank angle, there are theoretically two possibilities of making a steady turn, with two different A.O.A.s and load factors ;

c) the rate of descent, or height loss per turn is very sensitive to α at low A.O.A.

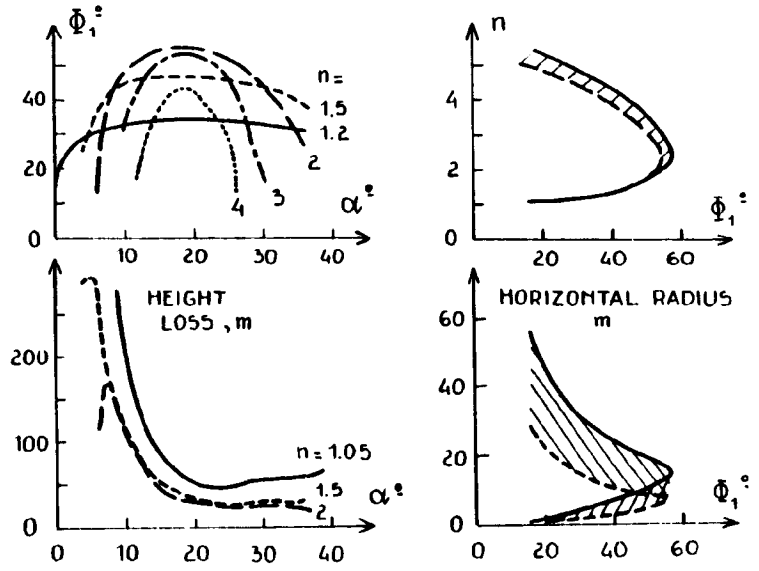

Fig. 22 – Typical wing turn performance. *Performance envelope of all gliders known.*

STRUCTURE

In France, in the early years of hang-gliding, no evidence of structural failures was obtained. Some stresses were measured in flight or in the tunnel, and no critical figure was found. This was attributed to practical knowledge of the manufacturers, and also poor performance (mainly diving speed) of the gliders. Also, the demonstration made about turning performance was anything but alarming. But the gliders on the market got improved performances, and some problems were encountered. The investigation was started by an analysis of the load factors which may be applied in real flight. It appeared that a value of 2 is difficult to overshoot in steady turn, whereas a symmetric pull-out (push-out) would perhaps reach 3 or more. A typical pull-out is shown on figure 23.

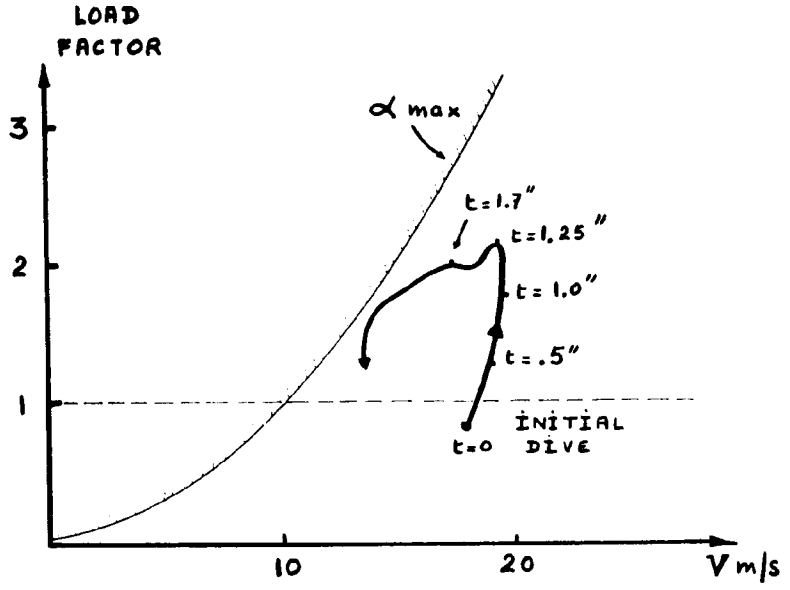

Fig. 23 – Time-history of a dive recovery.

Then structure calculations began separately on leading-edges, keels, and cross-spars. That isostatic technique did not succeed because it supposed a mandatory partition of the aerodynamic efforts. The real phenomenon required a more global approach, which was allowed by the use of a finite element program [10]. Figure 24 shows a typical result, giving both the stresses and displacements. As expected, the use of the program is easy, but the distribution of aerodynamic loading is somewhat arbitrary. An effective help was found in using sail shape identification with photography in the tunnel. Close comparison with some flight results and many ground tests gave credit to the method.

Key results are given in figure 25. But the prediction of breaking loads remains difficult, because of the scatter found in ground tests. That result will lead to a fairly high safety factor if the calculation is accepted as a design tool.

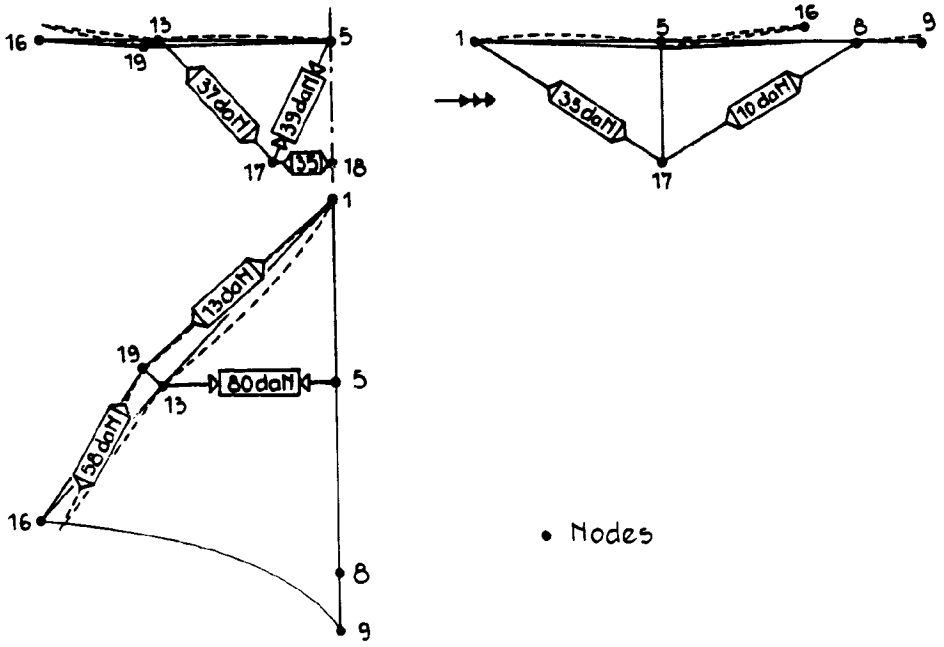

Fig. 24 – Finite elements stresses and displacements as provided by the computer. Swallowtail. Cruise A.O.A.

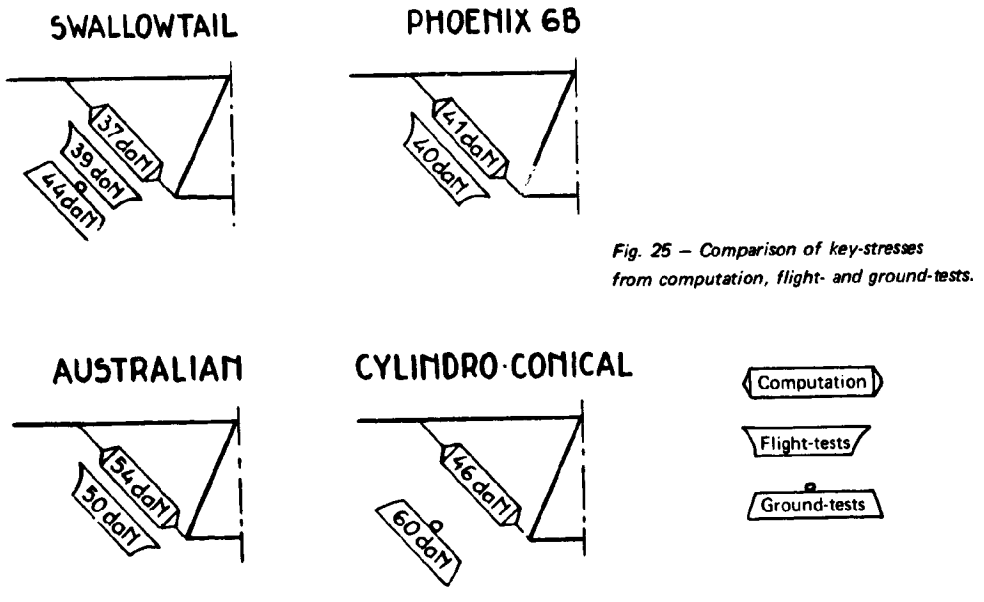

Fig. 25 – Comparison of key-stresses from computation, flight- and ground-tests.

CONCLUSION

The study was most interesting because of its many aspects and the possibility of constant crosschecking between flight and theory. As aircraft, Rogallo wings are really remarkable vehicles. The physical properties of a fabric profile which is self-adapting its own shape to A.O.A. provides a very wide flying envelope, and probably smoother losses of control. But these shape modifications may induce dangerous stability problems, which can be dominated by a good knowledge of aeroelastic effects. Several limits of the flying envelopes were determined, as shown on figures 26 to 31.

But the final aim of the study was a proposal of specifications. Although that question is very difficult to answer [11], it was established that a longitudinal stability criterion should rather refer to "control bar free" curves. But the choice of a minimum required value for $dF/d\alpha$ would be very inadequate because it would result in the acceptance of a few gliders which, being very stable, have a very poor maneuverability. A recommended solution might be to require neutral stability around cruise conditions (min. sink, and max. L/D) and an increasing positive stability at low A.O.A. At stall conditions, the safety problem does not lie in longitudinal stability which is fundamentally very positive, and the certificator's attention should be withdrawn, if possible.

The general problem of hang-gliders acceptance was broadened to the proposal of using two different tools, one for aerodynamics and one for structure, Considering that those accidents which are the consequences of aerodynamic defects result from abrupt discontinuities (mainly $C_{M\alpha}$ and $C_{M\beta}$), it was proposed to build a test vehicle, temporarily called AUTHOPUL (AUtomobile pour les Tests et l'HOmologation des Planeurs Ultra-Légers). This is far less precise than a wind-tunnel but it is in the financial range of the flying community, and would allow the removal of severe instabilities. The second tool is the finite element program for structure calculations, still cross-checked with ground tests.

But consideration of several significant accident reports showed evidence that the most important effort to be made for the safety of lang-gliders lies in the operational field rather than in navigability problems.

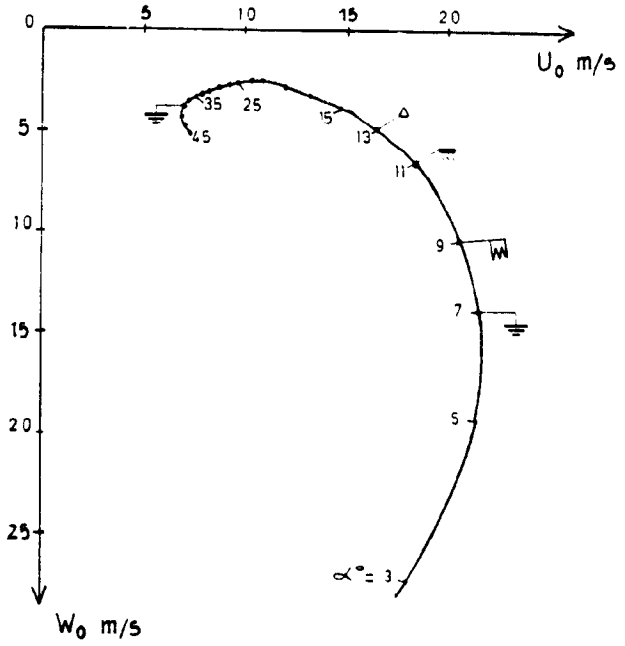

Fig. 26 – Standard.

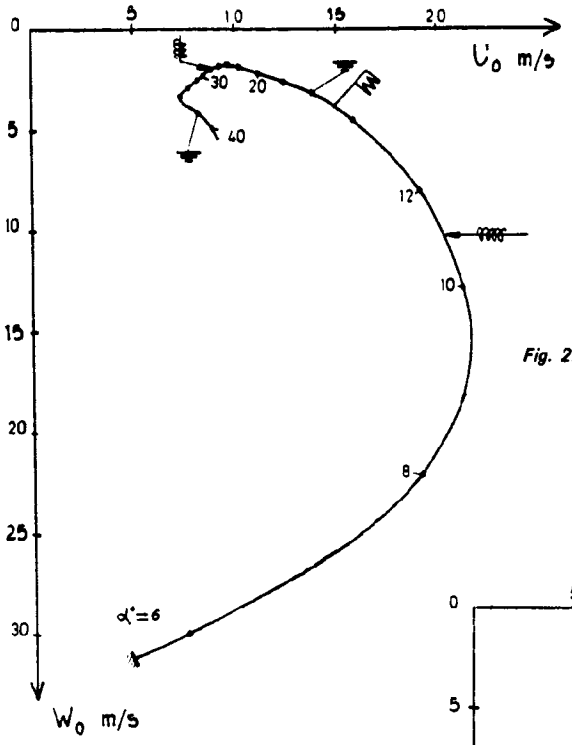

Fig. 27 – Swallowtail.

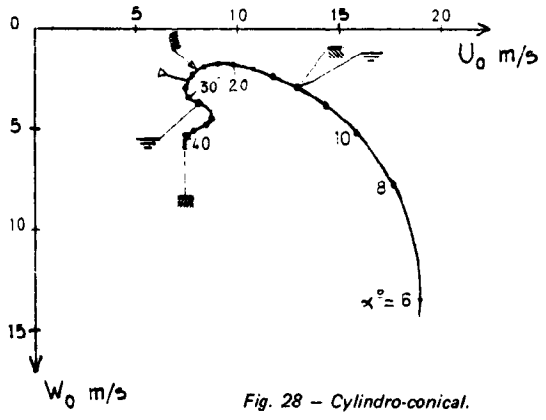

Fig. 28 – Cylindro-conical.

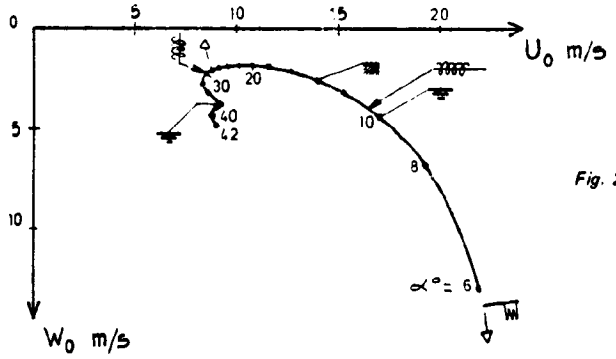

Fig. 29 – Phoenix 6B.

REPRODUCIBILITY OF THE
ORIGINAL PAGE IS POOR

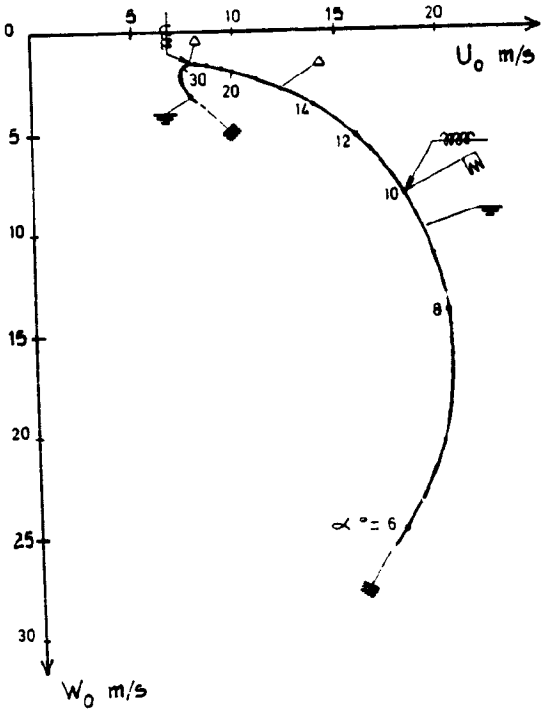

Fig. 30 – Australian shape.

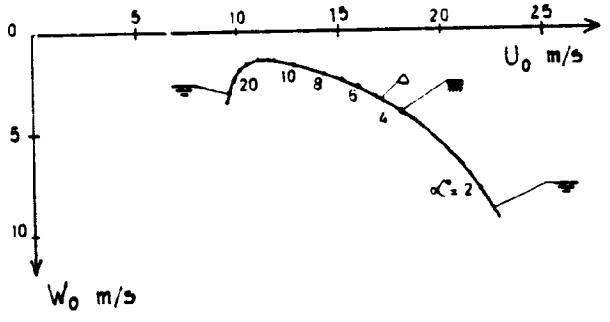

Fig. 31 – Fledgling I.

REFERENCES

[1] L. MALAVARD et ass. – *Propriétés calculées d' ailes en delta échancré ou non.* N.T. ONERA No 25 (1955).

[2] E.C. POLHAMUS – *Experimental and theoretical studies of the effects of camber and twist on the aerodynamical characteristics of parawings having nominal aspect ratio of 3 and 6.* NASA-TN-D-972 (1963).

[3] R.L. NAESETH and T.G. GAINER – *Low speed investigation of the effects of wing sweep on the aerodynamic characteristics of parawings.* NASA-TN-D-1957 (1963).

[4] H.R. MENDENHALL, S.B. SPANGLER and J.N. NIELSEN – *Investigation of methods for predicting the aerodynamic characteristics of two lobed parawings.* NASA-CR-1166 (1968).

[5] N. RIGAMONTI and H. PFLUGSHAUPT – *Untersuchung der stationären Flugzustäuche von zwei delta. Hängegleitern.* FO-1255.

[6] Ecole Nationale Supérieure de L'Aéronautique – *Caractéristiques aérodynamiques d'ailes Rogallo.* N.T.1/77.

[7] C.E. LIBBY and J.L. JOHNSON – *Stalling and tumbling of a radio-controlled parawing airplane model.* NASA-TN-D-2291.

[8] B. THWAITES – *Aerodynamic theory of sails.* Proc. Roy. Soc. Series A, vol. 261 (1961).

[9] J.N. NIELSEN – *Theory of flexible aerodynamic surfaces.* Journal of Applied Mechanics, No 63-AMP-29.

[10] C. LA BURTHE – Rapport Technique ONERA No 10/5134 S (1979).

[11] C. LA BURTHE – Rapport Technique ONERA No 8/5134 S et 9/5134 S (1978).

BIBLIOGRAPHY

P.G. FOURNIER and B.A. BELL – *Low subsonic pressure distribution on three rigid wings simulating paragliders with varied canopy curvature and leading edge sweep.* NASA-TN D-983.

S.F. HOERNER – *Résistance à l'avancement dans les fluides.* Gauthier Villars, Paris (1965).

R.T. JONES – *Properties of low-aspect ratio pointed wings at speeds below and above the speed of sound.* NACA report 835 (1946).

R. LEGENDRE – *Ecoulement transsonique autour d'ailes à forte fléche.* Publication ONERA No 53 (1952).

W.H. PHILLIPS – *Analysis and experimental studies of control of hang gliders.* The AIAA/MIT SSA Second International Symposium on the Science and Technology of Low-Speed and Motorless Flight, Cambridge, Mass, 1974.

F.M. ROGALLO et al. – *Preliminary investigation of a paraglider.* NASA T.N. D443 (1960).